Supplementary figures and tables for: A new model of the coupled carbon, nitrogen, and phosphorus cycles in the terrestrial biosphere (QUINCY v1.0; revision 1996)

Tea Thum[1], Silvia Caldararu[1], Jan Engel[1], Melanie Kern[1,2,3], Marleen Pallandt[1,2], Reiner Schnur[4], Lin Yu[1], and Sönke Zaehle[1,5]

[1]Max Planck Institute for Biogeochemistry, Hans-Knöll Str. 10, 07745 Jena, Germany
[2]International Max Planck Research School (IMPRS) for Global Biogeochemical Cycles, Jena, Germany
[3]Michael Stifel Center Jena for Data-driven and Simulation Science, Jena, Germany

Correspondence: Tea Thum (tthum@bgc-jena.mpg.de), Sönke Zaehle (szaehle@bgc-jena.mpg.de)

Table S1. The ten most important parameters (P) determining model sensitivity, measured as ranked partial correlation coefficient (RPCC), for each of the eight variables shown in Fig. 8 at the example of FR-Hes and reference to the respective parameter description table in the Supplementary Materials (T). The variables are GPP, net N/P mineralisation, vegetation and ecosystem C, as well as leaf C:N:P. The parameter names are color-coded, the red color is referring to photosynthesis related parameter, blue to soil biogeochemistry, cyan to vegetation growth and dynamics and black to water balance.

	GPP			Φ_{NH_4}			Φ_{PO_4}			**Leaf C:N**		
Rank	P	RPCC	T	P	RPCC	T	P	RPCC	T	P	RPCC	T
1	$T_{opt,decomp}$	-0.97	M2	$T_{opt,decomp}$	-0.93	23	$T_{opt,decomp}$	-0.89	M4	$T_{opt,decomp}$	0.96	M2
2	k_0^{struc}	-0.85	M7	$\eta_{C,litter\rightarrow fast}$	-0.58	M2	$K_{demand}^{half,N}$	0.67	M4	k_{rp}	0.80	M3
3	$\eta_{C,fast\rightarrow slow}$	-0.72	M2	k_{rp}	0.53	M3	$\eta_{C,litter\rightarrow fast}$	-0.65	M4	k_0^{struc}	-0.80	M7
4	$\eta_{C,litter\rightarrow fast}$	-0.71	M2	$\eta_{C,fast\rightarrow slow}$	-0.52	M2	$\chi_{leaf}^{N:P}$	-0.63	M7	sla	-0.70	M3
5	τ_{slow}^{base}	-0.63	M2	τ_{slow}^{base}	-0.50	M2	$\eta_{C,fast\rightarrow slow}$	-0.61	M4	$\eta_{C,litter\rightarrow fast}$	0.68	M4
6	sla	-0.58	M7	k_{resorb}^{leaf}	-0.41	M3	$\chi_{SOM_{slow}^{C:N}}$	0.36	M4	$\eta_{C,fast\rightarrow slow}$	0.65	M4
7	$T_{opt,nit}$	0.55	M2	$K_{demand}^{half,N}$	0.18	M4	k_{rp}	0.40	M3	τ_{slow}^{base}	0.59	M4
8	v_{cmax}^{n}	0.53	M2	sla	-0.36	M7	τ_{slow}^{base}	-0.37	M4	v_{cmax}^{n}	0.52	M2
9	τ_{fine_root}	0.49	M7	$\chi_{leaf}^{C:N}$	-0.35	M3	$\chi_{SOM_{slow}^{N:P}}$	0.36	M4	k_{latosa}	0.51	M7
10	$v_{max,NH_4\|NO_3}$	0.22	M7	$\chi_{root}^{C:N}$	0.33	M3	k_{resorb}^{leaf}	-0.33	M3	$T_{opt,nit}$	-0.50	M2

Table S1. The ten most important parameters (P), continued.

	Leaf N:P			**Veg. C**			**Total C**		
Rank	P	RPCC	T	P	RPCC	T	P	RPCC	T
1	$\chi_{root}^{N:P}$	0.94	M3	k_0^{struc}	-0.86	M2	$T_{opt,decomp}$	-0.90	M2
2	$K_{demand}^{half,N}$	-0.93	M4	k_{rp}	-0.78	M3	k_{rp}	-0.89	M3
3	$\chi_{leaf}^{N:P}$	0.84	M3	$f_{resp,maint}^{non-woody}$	-0.59	M2	k_0^{struc}	-0.71	M7
4	$\chi_{wood}^{N:P}$	0.65	M3	v_{cmax}^{n}	0.56	M2	k_{latosa}	-0.64	M7
5	k_{rp}	-0.50	M3	$\chi_{wood}^{N:P}$	-0.54	M3	$\eta_{C,fast\rightarrow slow}$	-0.51	M2
6	$T_{opt,decomp}$	0.45	M2	$\chi_{root}^{C:N}$	-0.52	M7	$\eta_{C,litter\rightarrow fast}$	-0.47	M2
7	v_{max,PO_4}	-0.33	M7	k_0^{chl}	-0.47	M7	τ_{slow}^{base}	-0.43	M2
8	sla	0.24	M3	k_{latosa}	-0.45	M3	$f_{resp,maint}^{non-woody}$	-0.42	M2
9	k_{latosa}	-0.19	M3	τ_{fine_root}	0.41	M7	τ_{fine_root}	0.42	M2
10	$k_{pref,runoff}$	0.17	M6	$T_{opt,decomp}$	-0.40	M4	$\chi_{wood}^{C:N}$	-0.41	M3

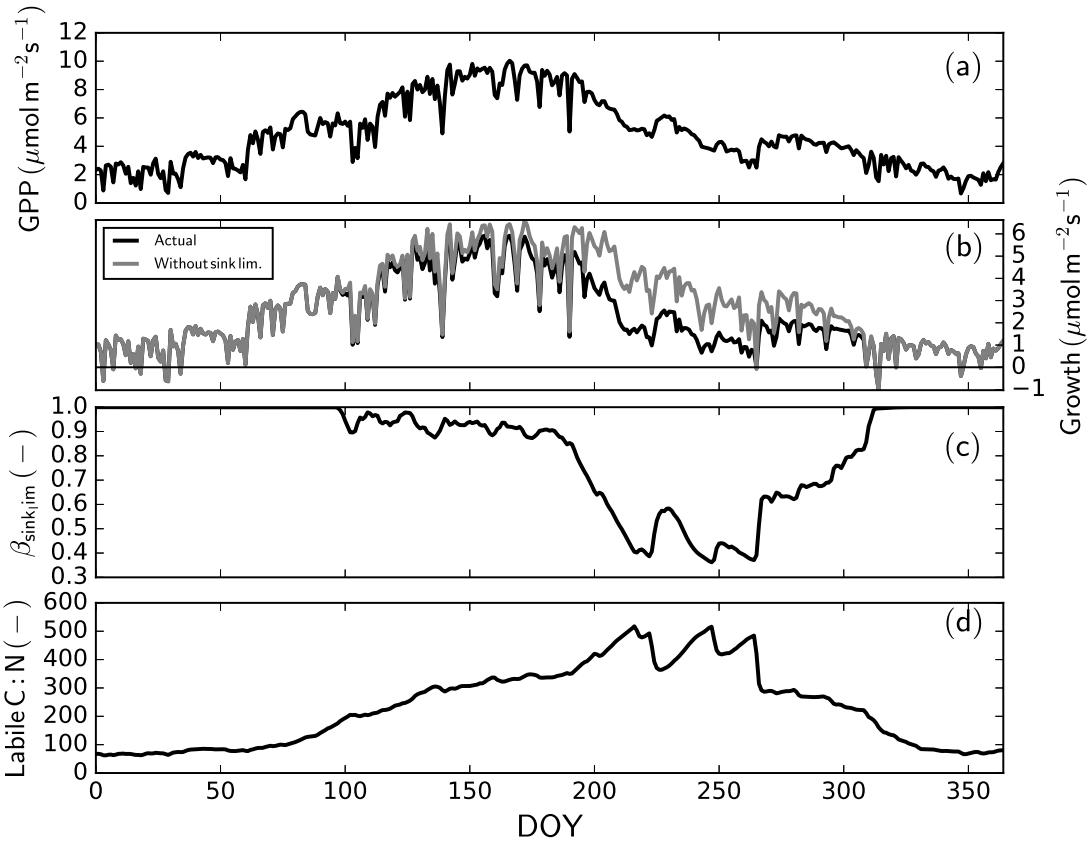

Figure S1. Effect of sink limitation on simulated photosynthesis at the example of the evergreen broadleaf forest site IT-Cpz. Daily GPP (a), growth (b), the sink limitation scalar ($\beta^{ps}_{sinklim}$) (c) and C:N of labile pool. The sink limitation is caused by high labile pool C:N ratio reducing the realised growth rate, which then provides a negative feedback to the photosynthesis.

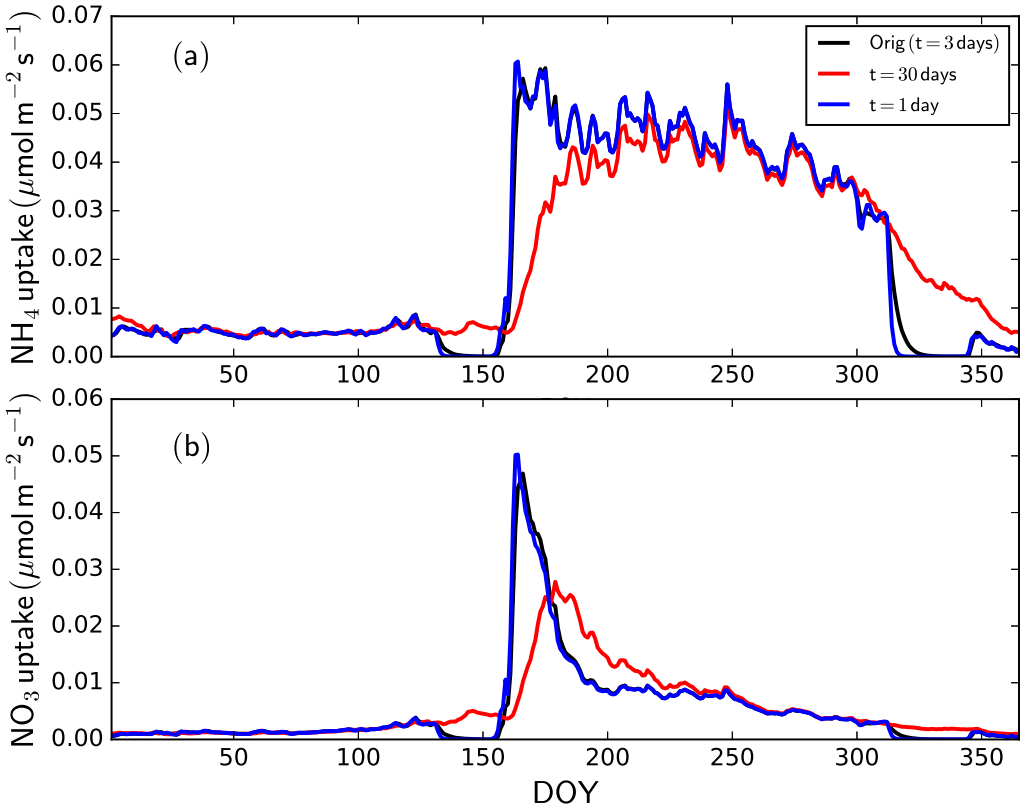

Figure S2. Effect of using a lagged response to calculate fluxes, at the example of the effect of plant nutrient demand on plant nutrient uptake in the temperate broadleaved deciduous forest of DK-Sor. Shown is the effect of altering the lag time of the demand for nutrient uptake (τ_{mavg}^{uptake}) on the nitrogen uptake fluxes for one year. The different colors respond to different lag times as explained in the legend.

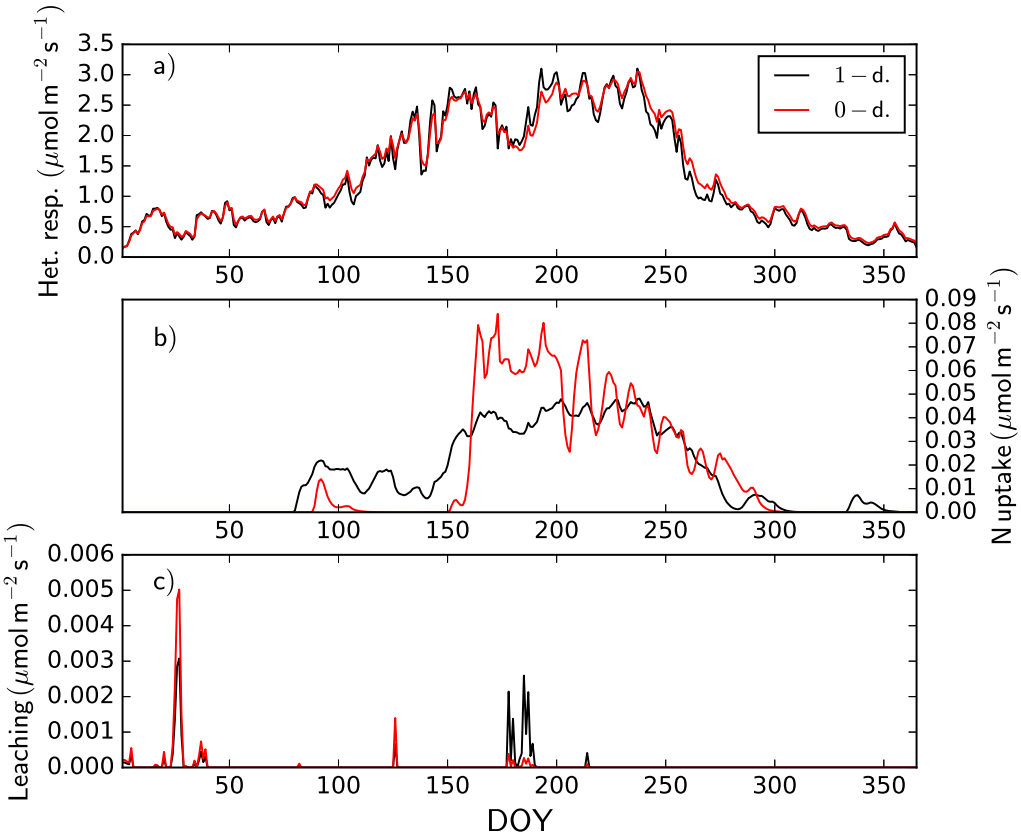

Figure S3. Effect of explicitly representing the vertical profile of the soils (1D), compared to a lumped OD approach. Displayed are the daily heterotrophic respiration (a) plant nitrogen uptake (b), and nitrogen leaching below the rooting zone (c) for one year at the needle-leaved evergreen forest sute of FI-Hyy.

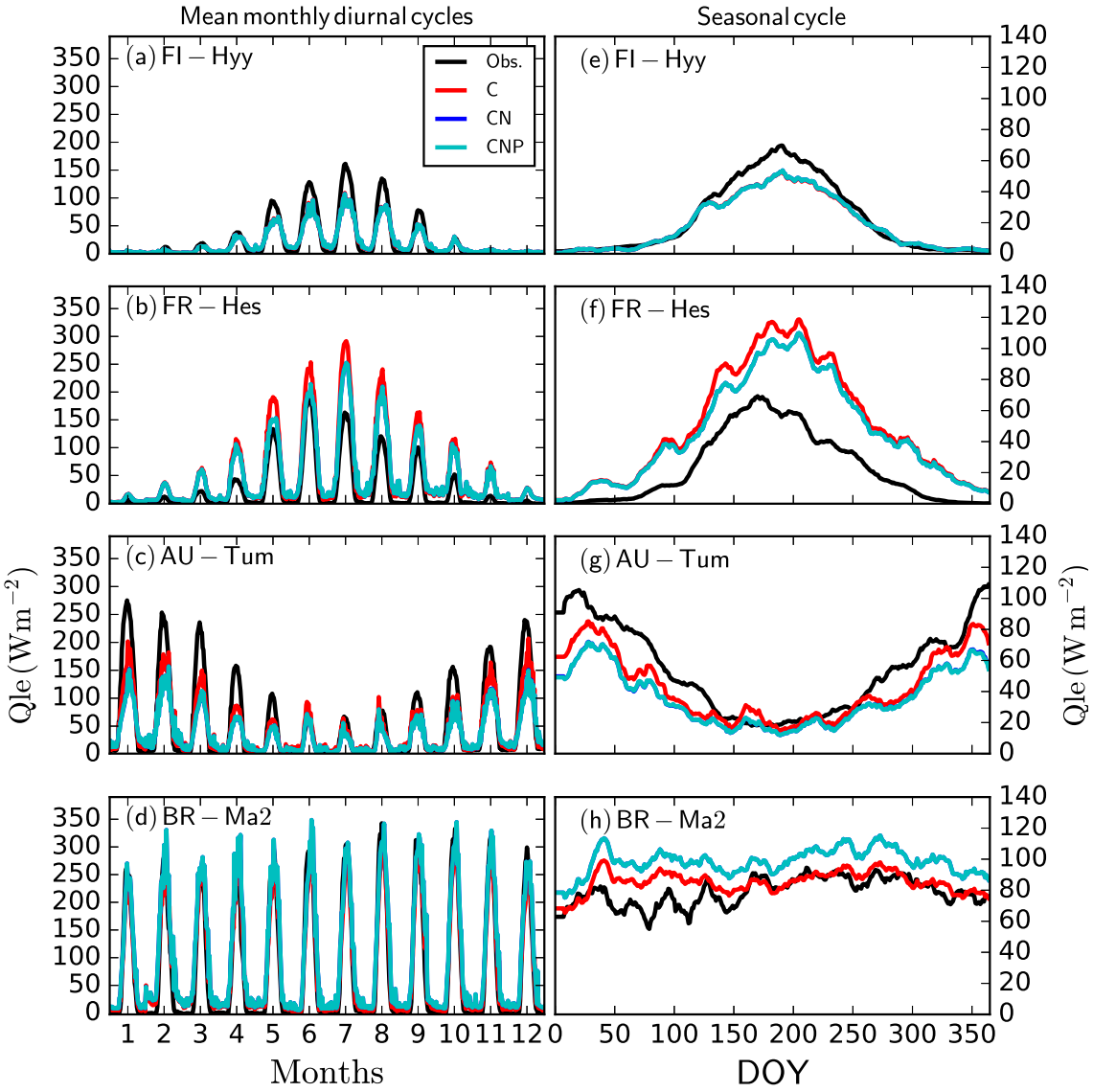

Figure S4. Simulated and observed mean monthly diurnal (a, b, c, d) and seasonal (e, f, g, h) cycles of latent heat flux (Q_{le}) at four FLUXNET sites (FI-Hyy, FR-Hes, AU-Tum, BR-Ma2. 'Obs' correspond to micrometeorological observations. 'C', 'CN' and 'CNP' refer to the model simulations with C, C&N and C&N&P options enabled. Seasonal cycles have been smoothed by a 16-day running mean.

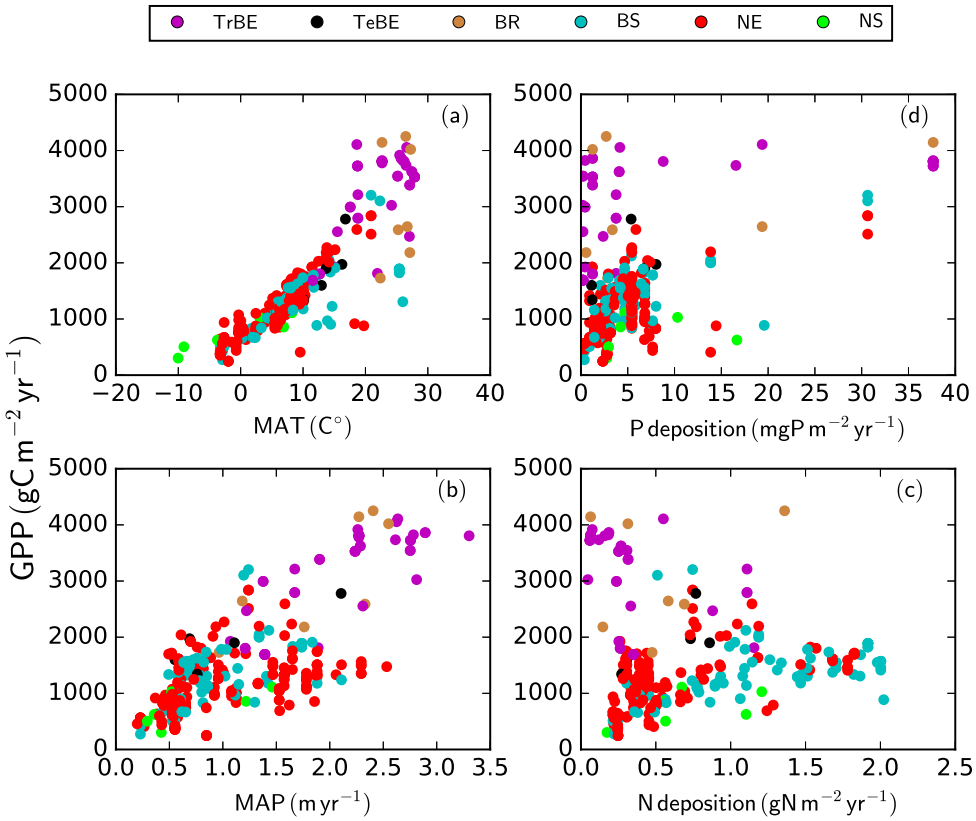

Figure S5. The GPP at the GFDB sites as a function of mean annual temperature (a), mean annual precipitation (b), nitrogen deposition (c) and phosphorus deposition (d). The PFT abbreviations are explained in Table 1.

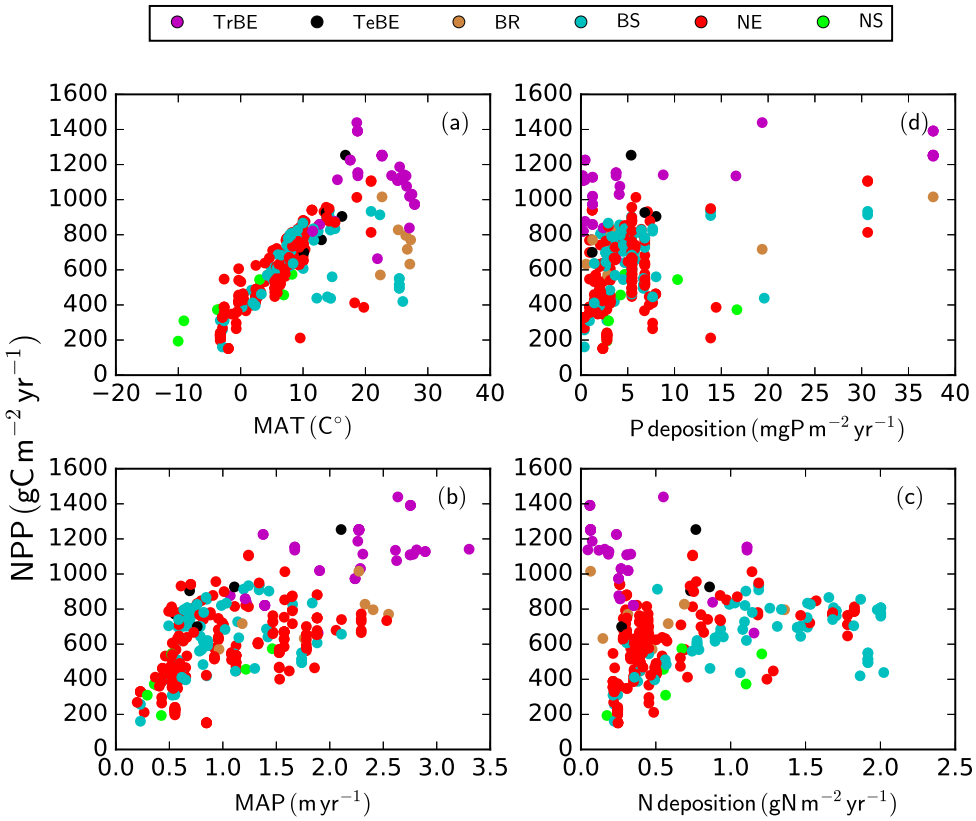

Figure S6. The NPP at the GFDB sites as a function of mean annual temperature (a), mean annual precipitation (b), nitrogen deposition (c) and phosphorus deposition (d). The PFT abbreviations are explained in Table 1.

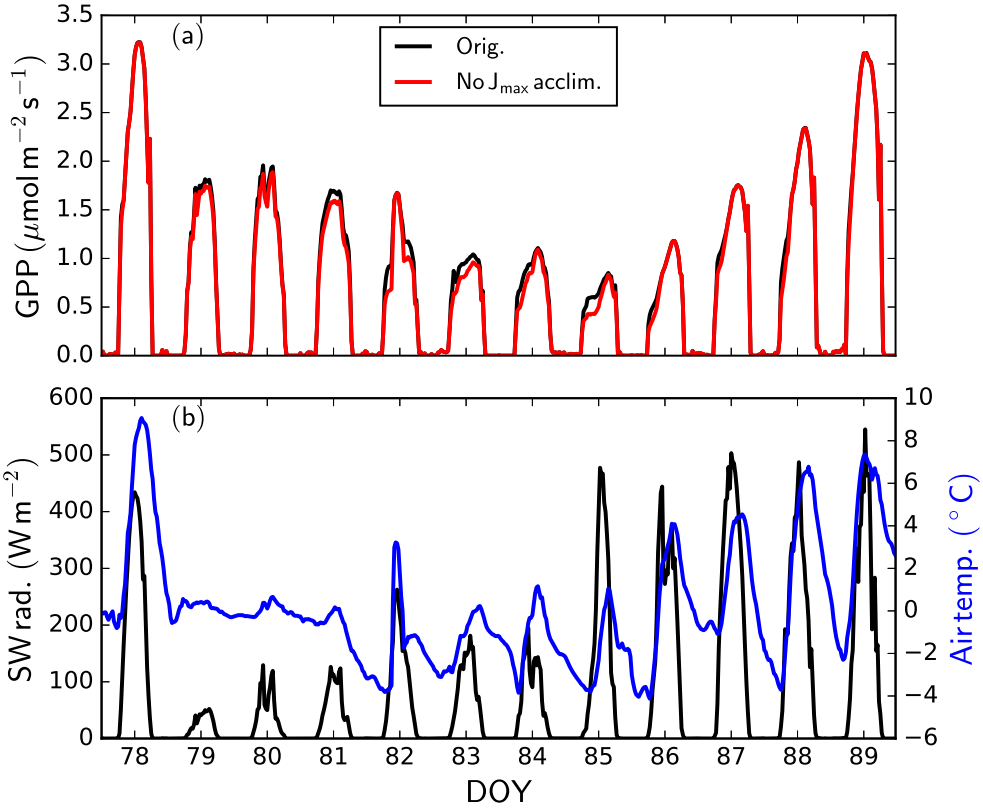

Figure S7. Effect of letting the temperature optimum of Jmax, the maximum electron-transport rate for the calculation of photosynthesis, acclimate to growth temperature (black), or not (red). The simulated diurnal cycles of GPP (a) and shortwave radiation (in black) and air temperature (in blue) (b) at FI-Hyy in 2002 for twelve days.

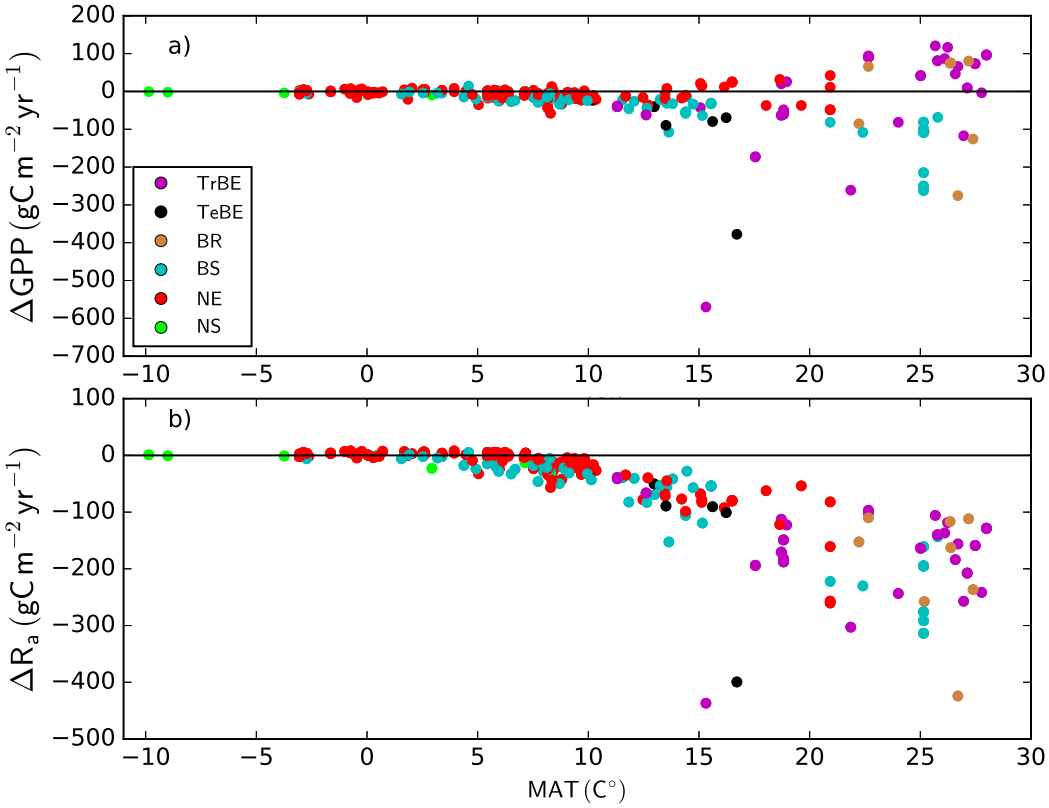

Figure S8. The residuals of averaged annual GPP (a) and autotrophic respiration (b), when the results without acclimation of maintenance respiration have been substracted from the original model simulations.

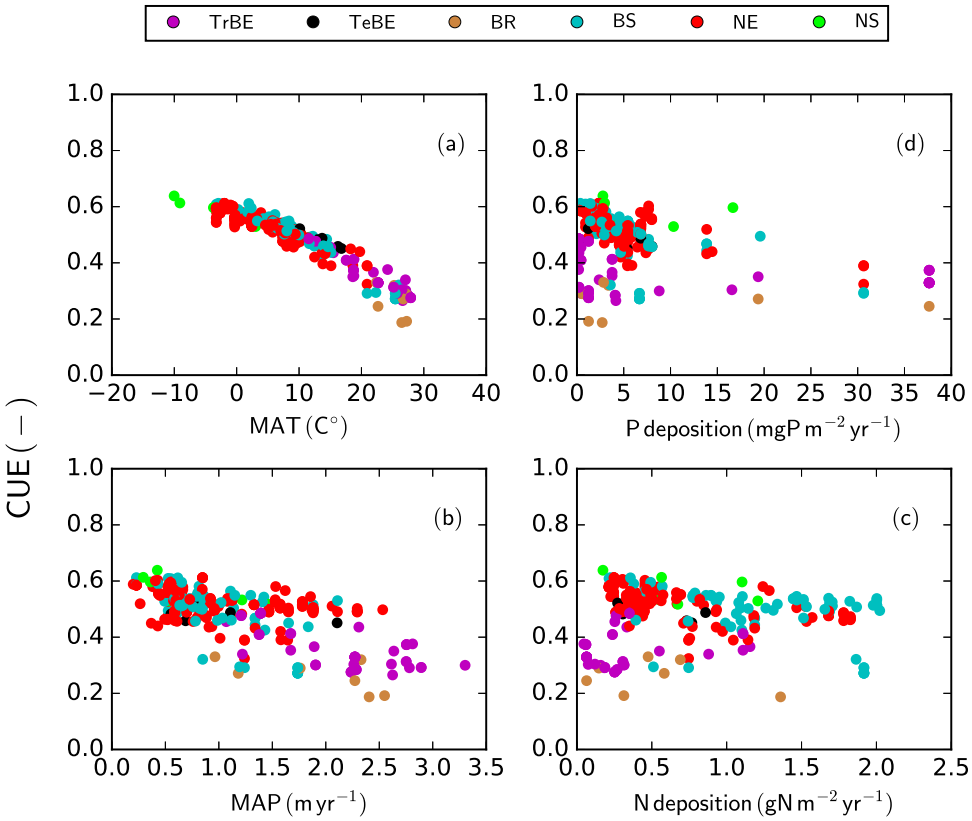

Figure S9. The CUE at the GFDB sites as a function of mean annual temperature (a), mean annual precipitation (b), nitrogen deposition (c) and phosphorus deposition (d). The PFT abbreviations are explained in Table 1.

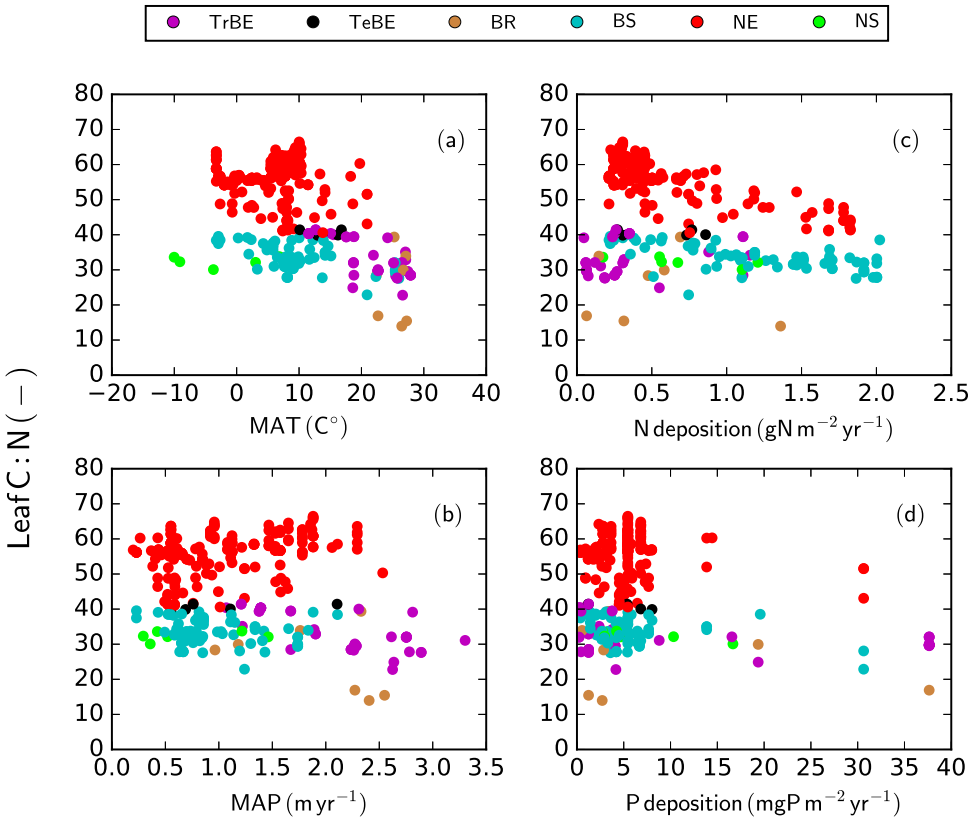

Figure S10. The leaf C:N at the GFDB sites as a function of mean annual temperature (a), mean annual precipitation (b), nitrogen deposition (c) and phosphorus deposition (d).

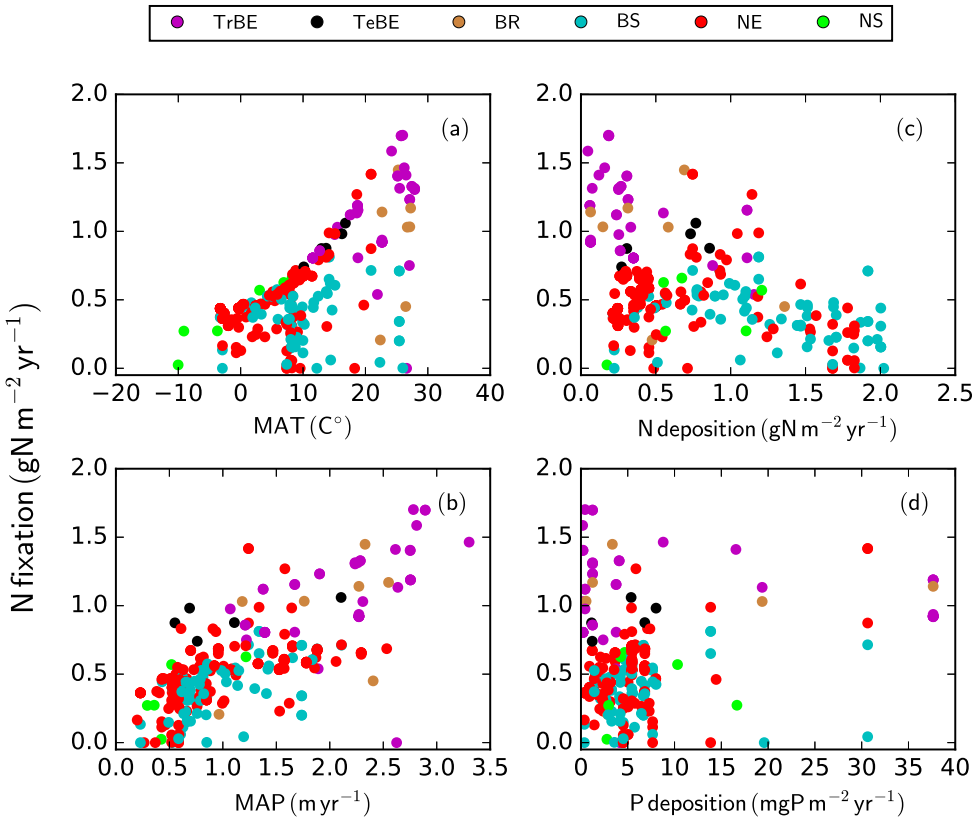

Figure S11. The nitrogen fixation at the GFDB sites as a function of mean annual temperature (a), mean annual precipitation (b), nitrogen deposition (c) and phosphorus deposition (d).

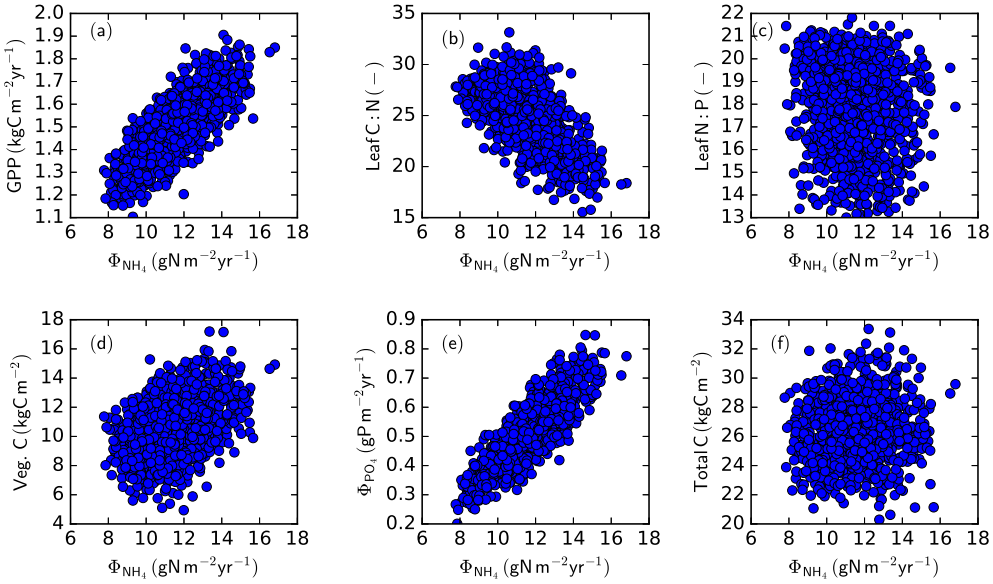

Figure S12. The GPP (a), leaf C:N (b), leaf P:N (c), vegetation carbon (d), phosphorus mineralization (e) and total ecosystem carbon (f) as function of nitrogen mineralization at FR-Hes for different parameter combinations from LHS.